# Testing the FLRW metric with Hubble and transverse BAO measurements

Min Wang,[1] Xiangyun Fu,[1,*] Bing Xu,[2,†] Ying Yang,[1] and Zhaoxia Chen[1]
[1]*Department of Physics, Key Laboratory of Intelligent Sensors and Advanced Sensor Materials, Hunan University of Science and Technology, Xiangtan, Hunan 411201, China*
[2]*School of Electrical and Electronic Engineering, Anhui Science and Technology University, Bengbu, Anhui 233030, China*

(Received 11 January 2023; accepted 13 October 2023; published 6 November 2023)

The cosmological principle is one of the fundamental assumptions of the standard model of cosmology (SCM), and it allows us to describe cosmic distances and clocks by using the Friedmann-Lemaître-Roberton-Walker (FLRW) metric. Thus, it is essential to test the FLRW metric with cosmological observations to verify the validity of the SCM. In this work, we perform tests of the FLRW metric by comparing the observational comoving angles between the Hubble $H(z)$ and the transversal baryon acoustic oscillation (BAO) measurements. The Gaussian process is employed to reconstruct the Hubble $H(z)$ measurements and the angular diameter distance (ADD) from the transversal BAO data. A nonparametric method is adopted to probe the possible deviations from the FLRW metric at any redshift by comparing the comoving distances from the reconstructed Hubble $H(z)$ measurements with the ADD reconstructed from the transversal BAO data. Then, we propose two types of parametrizations for the deviations from the FLRW metric, and test the FLRW metric by using the priors of specific sound horizon scales. To avoid the bias caused by the prior of a specific sound horizon scale, we perform the consistency test with a flat prior of the sound horizon scale. We find that there is a concordance between the FLRW metric and the observational data by using parametric and nonparametric methods, and the parametrizations can be employed to test the FLRW metric in a new way independent of the sound horizon scale.

DOI: 10.1103/PhysRevD.108.103506

## I. INTRODUCTION

In 1998, the unexpected dimming of type Ia supernova (SNIa) revealed the evidence of the accelerating expansion of the Universe for the first time [1,2]. In the frame of general relativity, a cosmic distribution of an exotic component with negative pressure, dubbed as dark energy, has been suggested to explain the accelerating expansion. In addition, a type of cold dark matter in the Universe is needed to explain the formation of the cosmic structure and galaxy dynamics. So far, the cosmological constant $\Lambda$ is the best candidate to explain the so-called dark energy. Thus, the standard model of cosmology (SCM), a flat cosmological constant $\Lambda$ cold dark matter ($\Lambda$CDM) model, has been established successfully to explain cosmological observations from the cosmic microwave background (CMB) [3], SNIa luminosity distances [4], as well as the clustering and weak lensing of the large-scale structure [5–8]. The SCM scenario is based upon two fundamental assumptions. One is that general relativity can be considered as the underlying theory of gravity. The other is that the Universe is statistical homogeneity and isotropy at large scales, also known as the cosmological principle (*CP*). In modern cosmology, the *CP* is formulated as follows: at suitably large scales, the average evolution of the Universe is exactly governed by the Friedmann-Lemaître-Robertson-Walker (FLRW) metric [9]. The homogeneous $\Lambda$CDM model is a highly successful model that is compatible with almost all observations up to now. However, the SCM faces the challenges of the Hubble tension [10], fine-tuning problem [11], and cosmic coincidence problems [12,13]. The Hubble tension comes from the discrepancy between local measurements based on Cepheids and SNIa [14] and analysis of the CMB [3] in the framework of the $\Lambda$CDM model. These problems imply that there is a potential departure from the SCM, and the $\Lambda$CDM model needs further adjustments [15]. An effective way to support or exclude the $\Lambda$CDM paradigm is to verify the validity of the FLRW metric through new methods and various astronomic observations.

Maartens first proposed that homogeneity means a consistency relation between the angular diameter distances and comoving distances in the FLRW universe [16]. Any violation of the consistency relation implies a non-FLRW universe. Therefore, the consistency relations between cosmic distances and chronometers provide us with an

*Corresponding author: xyfu@hnust.edu.cn
†Corresponding author: xub@ahstu.edu.cn

 

opportunity to test the FLRW metric. Recently, Arjona and Nesseris introduced a function $\zeta'(z) = 1 - \theta_{H(z)}/\theta_{\rm BAO}$ to define the possible deviations from the FLRW metric, and tested cosmic homogeneity by comparing the Hubble $H(z)$ measurements from the clustering and radial baryon acoustic oscillation (BAO) data with the transversal BAO measurements [17]. Here, the $\theta_{H(z)}$ and $\theta_{\rm BAO}$ denote comoving angles from the Hubble $H(z)$ and transversal BAO measurements, respectively. The value of function $\zeta'(z)$ at any redshift was obtained with the method of genetic algorithms. Using the sound horizon scale based on ΛCDM model, they found that both reconstructions are consistent with the flat ΛCDM model at the $1\sigma$ confidence level (CL) and at $2\sigma$ CL, respectively. Then, Bengaly reconstructed the function $\zeta'(z)$ with the Gaussian process and tested the consistency relation by comparing the 18 radial BAO data points with transversal BAO data [18]. A mild deviation of the FLRW metric was obtained at $3.5\sigma$ CL in the relatively low redshift range $0.1 < z < 0.3$ under the priors of the SH0ES $H_0$ and the specific sound horizon scales $r_{\rm s}$ from the Sloan Digital Sky Survey (SDSS) data release 11 galaxies [19] and BAO measurements [20].

It is easy to see that both tests in Refs. [17,18] are dependent on the values of the present Hubble parameter $H_0$ and the sound horizon scale $r_{\rm s}$. It should be noted that the so-called fitting problem remains a challenge for BAO peak location as a standard ruler [21], although the BAO measurements are employed to analyze various cosmological parameters. In particular, Roukema *et al.* recently detected the environmental dependence of BAO location [22,23]. Moreover, Ding *et al.* and Zheng *et al.* pointed out a noticeable systematic difference between Hubble $H(z)$ measurements based on BAO and those obtained with differential aging techniques [24,25]. In addition, different sound horizon scales $r_{\rm s}$ and the present Hubble parameter $H_0$ are obtained from various observational data, such as, CMB observations [26,27], the SDSS data release 11 galaxies [19], and BAO measurements [20]. Any prior of $r_{\rm s}$ may bring bias on the test of the FLRW metric. Therefore, it is meaningful to test the FLRW metric with new methods independent of the sound horizon scales $r_{\rm s}$, which is the main motivation of this work.

We first test the FLRW metric by comparing the observational comoving angles from the Hubble $H(z)$ measurements with that from the transversal BAO data. The Hubble parameter $H(z)$ measurements are either obtained by the differential age method or by the determination of the BAO peak in the radial direction (hereafter referred to as radial BAO observations). The function $\zeta(z) = 1 - \theta_{\rm BAO}/\theta_{H(z)}$ is employed to quantify the possible deviation from the FLRW metric. To obtain the observed value of function $\zeta(z)$ at any redshift, the Gaussian process is employed to reconstruct the Hubble $H(z)$ measurements and the angular distances from the transversal BAO data. The results show that the best-fit values of function $\zeta(z)$ vary with redshift $z$. Then, we propose two general types of parametrizations for the function $\zeta(z)$, namely, P1: $\zeta(z) = \zeta_0(1+z)$ and P2: $\zeta(z) = \zeta_0/(1+z)$. Here, the nonzero constant $\zeta_0$ represents a possible deviation from the FLRW metric. We test the FLRW metric successively by using the priors of specific sound horizon scales $r_{\rm s}$ and a flat priors of $r_{\rm s}$. We show that the FLRW metric is consistent with the observational data, and the parametric method provides an effective way independent of the sound horizon scale $r_{\rm s}$ to test the consistency relation.

## II. DATA AND METHODOLOGY

### A. Observational data

The Hubble parameter $H(z)$ measurements in our analysis can be obtained by two interrelated methods. The first compilation comes from the differential age (DA) method proposed in Ref. [28], where the ages of early-type galaxies are compared with the same metallicity and separated by small redshift intervals. In general relativity, the Hubble parameter $H(z)$ can be also written as

$$H(z) = -\frac{1}{1+z}\frac{dz}{dt}, \tag{1}$$

where $dz/dt$ is measured using the 4000 Å break feature as function of redshifts. Thus, this approach directly measures the Hubble parameter by using spectroscopic dating of passive evolutionary galaxies to compare their ages and metallicities, providing $H(z)$ measurements in a cosmological model-independent method [29–37]. Here, the 31 cosmological model-independent data points are compiled in Table I. The second $H(z)$ compilation comes from the clustering of galaxies or quasars, being a direct probe of the Hubble expansion by determining the BAO peak in the radial BAO observations [38,39]. 18 Hubble $H(z)$ measurements of the radial BAO mode are compiled in Table II. It should be noted that the observed Hubble data from radial BAO mode are obtained with an underlying ΛCDM cosmological model. So, any method using Hubble data obtained from the radial BAO measurements is not completely cosmological model-independent.

The 15 transversal BAO measurements [19,49–52] are compiled in Table III, which were obtained using public data releases of the SDSS [53]. These measurements of the BAO scale can be obtained by using the angular 2-point correlation function, which involves only the angular separation $\theta$ between pairs, yielding information of the angular diameter distance (ADD) almost model-independently, provided that the comoving sound horizons is known [52]. The distributions of the transversal BAO measurements and Hubble $H(z)$ data are shown in Fig. 1.

TABLE I. 31 Hubble parameter measurements $H(z)$ obtained from the DA method (in units of km s$^{-1}$ Mpc$^{-1}$).

| $z$ | $H(z)$ | $\sigma_{H(z)}$ | Reference | $z$ | $H(z)$ | $\sigma_{H(z)}$ | Reference | $z$ | $H(z)$ | $\sigma_{H(z)}$ | Reference |
|---|---|---|---|---|---|---|---|---|---|---|---|
| 0.07 | 69 | 19.6 | [29] | 0.4 | 95 | 17 | [30] | 0.88 | 90 | 40 | [30] |
| 0.10 | 69 | 12 | [30] | 0.4004 | 77 | 10.2 | [32] | 0.9 | 117 | 23 | [30] |
| 0.12 | 68.6 | 26.2 | [29] | 0.4247 | 87.1 | 11.2 | [32] | 1.037 | 154 | 20 | [31] |
| 0.17 | 83 | 8 | [30] | 0.4497 | 92.8 | 12.9 | [32] | 1.3 | 168 | 17 | [30] |
| 0.1791 | 75 | 4 | [31] | 0.47 | 89 | 34 | [33] | 1.363 | 160 | 33.6 | [34] |
| 0.1993 | 75 | 5 | [31] | 0.4783 | 80.9 | 9 | [32] | 1.43 | 177 | 18 | [30] |
| 0.20 | 72.9 | 29.6 | [29] | 0.48 | 97 | 62 | [30] | 1.53 | 140 | 14 | [30] |
| 0.27 | 77 | 14 | [30] | 0.5929 | 104 | 13 | [31] | 1.75 | 202 | 40 | [30] |
| 0.28 | 88.8 | 36.6 | [29] | 0.6797 | 92 | 8 | [31] | 1.965 | 168.5 | 50.4 | [34] |
| 0.3519 | 83 | 14 | [31] | 0.7812 | 105 | 12 | [31] | | | | |
| 0.3802 | 83 | 13.5 | [32] | 0.8754 | 125 | 17 | [31] | | | | |

TABLE II. 18 Hubble parameter measurements $H(z)$ obtained from the radial BAO measurements (in units of km s$^{-1}$ Mpc$^{-1}$).

| $z$ | $H(z)$ | $\sigma_{H(z)}$ | Reference | $z$ | $H(z)$ | $\sigma_{H(z)}$ | Reference | $z$ | $H(z)$ | $\sigma_{H(z)}$ | Reference |
|---|---|---|---|---|---|---|---|---|---|---|---|
| 0.24 | 79.69 | 2.65 | [38] | 0.43 | 86.45 | 3.68 | [38] | 0.60 | 87.9 | 6.10 | [40] |
| 0.30 | 81.70 | 6.22 | [41] | 0.44 | 82.60 | 7.80 | [40] | 0.61 | 97.3 | 2.10 | [42] |
| 0.31 | 78.17 | 4.74 | [43] | 0.51 | 90.40 | 1.90 | [42] | 0.64 | 98.82 | 2.99 | [43] |
| 0.35 | 82.70 | 8.40 | [44] | 0.52 | 94.35 | 2.65 | [43] | 2.33 | 224.00 | 8.00 | [45] |
| 0.36 | 79.93 | 3.39 | [43] | 0.56 | 93.33 | 2.32 | [43] | 2.34 | 223.00 | 7.00 | [46] |
| 0.38 | 81.50 | 1.90 | [42] | 0.57 | 98.48 | 3.19 | [47] | 2.36 | 227.00 | 8.00 | [48] |

TABLE III. 15 transversal BAO measurements $\theta_{\mathrm{BAO}}$ (in deg) and their errors $\sigma_{\mathrm{BAO}}$ at redshift $z$. These data were obtained through public data publication using SDSS.

| $z$ | $\theta_{\mathrm{BAO}}$ | $\sigma_{\mathrm{BAO}}$ | Reference | $z$ | $\theta_{\mathrm{BAO}}$ | $\sigma_{\mathrm{BAO}}$ | Reference | $z$ | $\theta_{\mathrm{BAO}}$ | $\sigma_{\mathrm{BAO}}$ | Reference |
|---|---|---|---|---|---|---|---|---|---|---|---|
| 0.11 | 19.8 | 3.26 | [54] | 0.49 | 4.99 | 0.21 | [49] | 0.59 | 4.39 | 0.33 | [19] |
| 0.235 | 9.06 | 0.23 | [50] | 0.51 | 4.81 | 0.17 | [49] | 0.61 | 3.85 | 0.31 | [19] |
| 0.365 | 6.33 | 0.22 | [50] | 0.53 | 4.29 | 0.30 | [49] | 0.63 | 3.90 | 0.43 | [19] |
| 0.45 | 4.77 | 0.17 | [49] | 0.55 | 4.25 | 0.25 | [49] | 0.65 | 3.55 | 0.16 | [19] |
| 0.47 | 5.02 | 0.25 | [49] | 0.57 | 4.59 | 0.36 | [19] | 2.225 | 1.77 | 0.31 | [51] |

### B. Gaussian process

To test the consistency relation between the ADDs and comoving distances in the FLRW universe [16], the simplest way is to make the comparison between the radial and transversal angular mode at the same redshift [16,17]. In principle, given a comoving observed angle mode from the Hubble measurements, one should select the corresponding one from the transversal BAO data at the same redshift $z$ to test the FLRW metric. However, this condition usually cannot be met in recent astronomical observations.

The Gaussian process provides a powerful tool for the distribution of functions in a stochastic statistical process, and it has gained much attention in cosmology due to its ability to reconstruct cosmological data in a model-independent manner. The distribution of function value is a Gaussian at each point $x$, and the reconstruction consists of a mean function with Gaussian error bands. The function values at different points are correlated by the covariance kernel $k(x, x')$, which depends on the hyperparameters of $\sigma_f$ and $l$. The parameter $l$ represents roughly to the distance one needs to be moved in the input space before the function value changes significantly, and $\sigma_f$ denotes typical changes in the function value [55]. The hyperparameters play important role in determining the error bars of observation data. Both of the hyperparameters are optimized by the Gaussian process with the observed dataset. Different Gaussian process kernels have been used for the null test in Ref. [18], and the results showed that different choices for kernels of Gaussian process provided slightly more degenerate reconstruction which reduced the statistical significance of these deviations. The Gaussian process has been employed to make constraints on

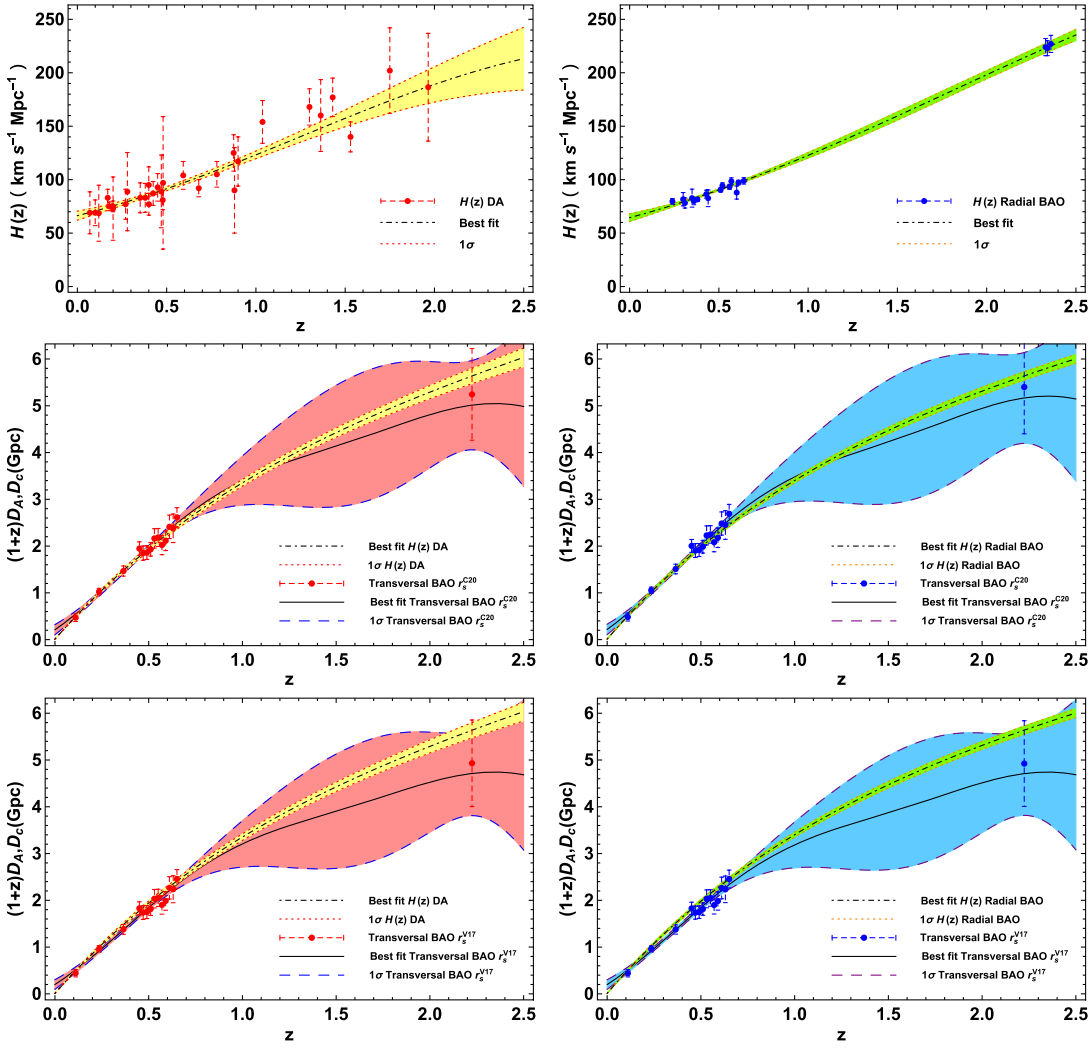


FIG. 1. Reconstructed $H(z)$ (top) and $D_{\rm C}(z)$ (middle and bottom) from Hubble measurements. The sample catalogs of the observed $(1+z)D_{\rm A}(z)$ distributions from the transversal BAO and the corresponding reconstructed curves (middle and bottom) with the $H_0^{\rm DA}$ (left panel) and $H_0^{\rm RB}$ (right panel) and the priors of $r_{\rm s}^{\rm C20}$ and $r_{\rm s}^{\rm V17}$.

cosmological constants with SNIa observation [56], to probe the micromotions of cosmic matter [57], to investigate the deceleration parameter and the duality-distance parameter [58], to constrain cosmological mixing parameters [59,60], and to infer the Hubble constant [61–63]. More recently, Zhang *et al.* used Bayes factors to evaluate the differences between different kernel functions by analyzing the cosmic chronometer data, SNIa, and gamma ray burst. The results showed that Bayes factors indicate no significant dependence of the data on each kernel [64].

To employ all of 15 transversal BAO measurements to probe the deviation from the FLRW metric, we reconstruct the Hubble measurements with the Gaussian process [65,66] to obtain the continuous $H(z)$ function. Therefore, for each transversal BAO data point, we can obtain the corresponding Hubble measurement with the same redshift from the reconstructed Hubble $H(z)$ function. In our analysis, following the results obtained from Ref. [64], we do not consider the impact of different kernels on the consistency relation, and adopt the general covariance kernel, namely the squared exponent [67]

$$k(x,x') = \sigma_f^2 \exp\left(-\frac{(x-x')^2}{2l^2}\right). \tag{2}$$

### C. Methodology

Following the approach to test the consistency relation as proposed in Refs. [16,17], deviations from the FLRW metric can be obtained by reconstructing the comoving distances ($D_{\rm C}$) from the Hubble $H(z)$ measurements and the ADD $D_{\rm A}$ from the transversal BAO observations. The Hubble $H(z)$ measurements in our analysis are obtained from the DA method and the radial BAO measurements, and they are listed in Tables I and II,

respectively. The comoving observed angle from the $H(z)$ data is given by

$$\theta_{H(z)} = \frac{r_s}{D_C(z)}, \tag{3}$$

and the same for the transversal BAO data,

$$\theta_{BAO} = \frac{r_s}{(1+z)D_A(z)}, \tag{4}$$

where $r_s$ is the sound horizon scale at the drag epoch, and the comoving distance $D_C$ can be written as

$$D_C(z) = c\int_0^z \frac{dz'}{H(z)}. \tag{5}$$

Using the Gaussian process, we first obtain the $H(z)$ in 2000 reconstruction bins in the redshift range $0 < z < 2.5$, and the results are shown in Fig. 1. The quantities of the present Hubble parameter $H_0$ from the reconstruction are shown as

$$H_0^{DA} = 66.3 \pm 4.22\ \mathrm{km\,s^{-1}\,Mpc^{-1}}, \tag{6}$$

$$H_0^{RB} = 64.4 \pm 3.56\ \mathrm{km\,s^{-1}\,Mpc^{-1}}, \tag{7}$$

here, the $H_0^{DA}$ and $H_0^{RB}$ denote the present Hubble parameters $H_0$ obtained from the method of differential age and radial BAO observations, respectively. The reconstructed results of $H_0$ are compatible with the observed constraints $H_0 = 67.0 \pm 0.9\ \mathrm{km\,s^{-1}\,Mpc^{-1}}$ obtained from the Hubble and SNIa data [39], and are a little less than the results $H_0 = 67.2 \pm^{1.2}_{1.0}\ \mathrm{km\,s^{-1}\,Mpc^{-1}}$ obtained from Dark Energy Survey Year 1 clustering combined with BAO and big bang nucleosynthesis [68].

We used the trapezoidal rule to numerically integrate the reconstructed $H(z)$, and obtain the comoving distance [18,60]

$$D_{C,i} = c\int_0^z \frac{dz'}{H(z')} \approx \frac{c}{2}\sum_{i=1}^{N}(z_{i+1}-z_i)\left[\frac{1}{H_{(z_{i+1})}} + \frac{1}{H_{(z_i)}}\right]. \tag{8}$$

The uncertainty of the $D_{C,i}$ obtained from reconstruction $H(z_i)$ is given by

$$\sigma_{D_{C,i}} = \frac{c}{2}(z_{i+1}-z_i)\left[\frac{\sigma^2_{H_{i+1}}}{H^4_{i+1}} + \frac{\sigma^2_{H_i}}{H^4_i}\right]^{1/2} \tag{9}$$

The integration in Eq. (8) is performed along the evenly spaced-out 2000 bins over the redshift range $0 < z < 2.5$, rather than over the inhomogeneous Hubble $H(z)$ measurements. The reconstructed $D_C(z)$ from the observed Hubble $H(z)$ measurements are shown in Fig. 1.

To obtain the ADD $D_A$ from the transversal BAO data, a sound horizon at radiation drag $r_s$ should be determined from the astronomic observations. The quantity of the sound horizon scale $r_s$ can be calibrated at $z > 1000$ from CMB observations and theoretical assumptions, i.e., $r_s = 147.33 \pm 0.49$ Mpc and $r_s = 152.30 \pm 1.3$ Mpc from the most recent Planck [26] and WMAP9 [27] measurements, respectively. At the relative low redshift, Carvalho *et al.*, made constraint on $r_s$ by using the SDSS data release 11 galaxies and a prior on the matter density parameter given by the SNIa data (hereafter referred to as $r_s^{C20}$) [19],

$$r_s^{C20} = 107.4 \pm 1.7h^{-1}\,\mathrm{Mpc}. \tag{10}$$

It should be noted that the measurement of $r_s^{C20}$ is model-dependent, since it was estimated by fitting the flat ΛCDM model to the transverse BAO data. Here, $h$ can be obtained from the following expression

$$H_0 = 100h\,\mathrm{km\,s^{-1}\,Mpc^{-1}}. \tag{11}$$

Verde *et al.* also obtained constraints on the length of the low-redshift standard ruler (referred to as $r_s^{V17}$)

$$r_s^{V17} = 101.0 \pm 2.3h^{-1}\,\mathrm{Mpc}, \tag{12}$$

when using SNIa and BAO measurements [20]. In this work, to avoid the bias caused by the different values of $H_0$ between the Hubble measurements and the transversal BAO observations, we use the corresponding value of $H_0$ reconstructed from the Hubble data and the sound horizon scales $r_s^{C20}$ and $r_s^{V17}$ at relative low redshift to derive the ADD $D_A$.

Then, using the Gaussian process, we reconstruct the ADD $D_A(z)$ as a smooth function of redshift $z$ from the transversal BAO data with the different priors of $r_s$ and $H_0$, and the results are shown in Fig. 1. From this figure, it can be seen that, at the same redshift, the value of $D_A$ obtained from the prior $r_s^{C20}$ is larger than that obtained from $r_s^{V17}$, since $r_s^{C20} > r_s^{V17}$ for the same value of $H_0$.

Following the approach proposed by Refs. [16,17], we can search for the possible deviations from the FLRW universe by comparing the $D_C$ obtained from the $H(z)$ measurements with the $D_A$ from transversal BAO observational data in the following expression,

$$\zeta(z) = 1 - \frac{\theta_{BAO}}{\theta_{H(z)}} = 1 - \frac{D_C(z)}{(1+z)D_A(z)}. \tag{13}$$

Here, the observational ADD $D_A(z)$ and comoving distances $D_C(z)$ can be obtained from the transversal BAO measurements and the reconstructed $H(z)$ measurements. Any violation from $\zeta(z) = 0$ in Eq. (13) implies a non-FLRW universe. The observed $\zeta_{obs}(z)$ can be obtained from Eq. (13), and the corresponding error of $\zeta_{obs}(z)$ is

$$\sigma^2_{\zeta_{\rm obs}} = \frac{D_{\rm C}^2}{(1+z)^2 D_{\rm A}^2}\left[\left(\frac{\sigma_{D_{\rm A}(z)}}{D_{\rm A}(z)}\right)^2 + \left(\frac{\sigma_{D_{\rm C}(z)}}{D_{\rm C}(z)}\right)^2\right]. \quad (14)$$

Here, $\sigma_{D_{\rm C}}$ can be obtained from the Hubble parameter with Equ. (9). $\sigma_{D_{\rm A}}$ is obtained with

$$\sigma^2_{D_{\rm A}} = D_{\rm A}^2\left[\left(\frac{\sigma_{r_{\rm s}}}{r_{\rm s}}\right)^2 + \left(\frac{\sigma_{\theta_{\rm BAO}}}{\theta_{\rm BAO}}\right)^2\right], \quad (15)$$

and variable $\theta$ needs to be converted from degrees to radians.

Then we can obtain the function $\zeta(z)$ with a nonparametric method at any redshifts by comparing the reconstructed $D_{\rm A}$ with the reconstructed $D_{\rm C}$ at the same redshift, and show the results in Fig. 2.

As seen from Fig. 2, the best value of a function $\zeta(z)$ is redshift dependent. Therefore, the function $\zeta(z)$ can be parametrized in different forms. It is well known that parametrized method plays an important role in testing the cosmic distance duality relation [69–73] and cosmic opacity [74–76]. In our analysis, for a manageable one-dimensional phase space and good sensitivity to observational data, we consider the following two parametrization forms. One is inversely proportional to the cosmic scale factor $a = 1/(1+z)$,

$$\text{P1}: \zeta(z) = \zeta_0(1+z), \quad (16)$$

and the other is proportional to the cosmic scale factor $a$,

$$\text{P2}: \zeta(z) = \zeta_0/(1+z), \quad (17)$$

where $\zeta_0$ is a constant parameter and represents possible deviation from the FLRW metric. Then, we can constrain the parameter $\zeta_0$ by comparing the reconstructed comoving distances $D_{\rm C}$ from Hubble $H(z)$ measurements with the angular distances $D_{\rm A}$ from the transversal BAO data at the same redshift. To match the observed $D_{\rm A}$ with the $D_{\rm C}$ at the same redshift, the values of $D_{\rm C}$ are obtained from the reconstructed comoving distances at the redshift of the transversal BAO measurements. Thus, all 15 available observed data of transversal BAO can be employed to test the FLRW metric. Therefore, $\chi^2$ is given by

$$\chi^2(\zeta_0) = \sum_i^N \frac{[\zeta(z) - \zeta_{{\rm obs},i}(z)]^2}{\sigma^2_{\zeta_{{\rm obs},i}}}. \quad (18)$$

Here, $N$ represents the number of the transversal BAO data points, and $N = 15$. The free parameter is $\zeta_0$, and the number of the degree of freedom used to perform the fitting procedure is 1. The reduced $\chi^2$ can obtained with $\chi^2_{\rm red} = \chi^2_{\rm min}/(N-1)$. The constraints on parameter $\zeta_0$ are shown in Fig. 3 and Table IV.

It is obvious to see that the results obtained from the nonparametric and parametric methods are dependent on the priors on the sound horizon scale. To test the FLRW metric independent of the sound horizon scale $r_{\rm s}$, we consider a fiducial value of $r_{\rm s}$ as a nuisance parameter to determine the ADD $D_{\rm A}$ from transversal BAO

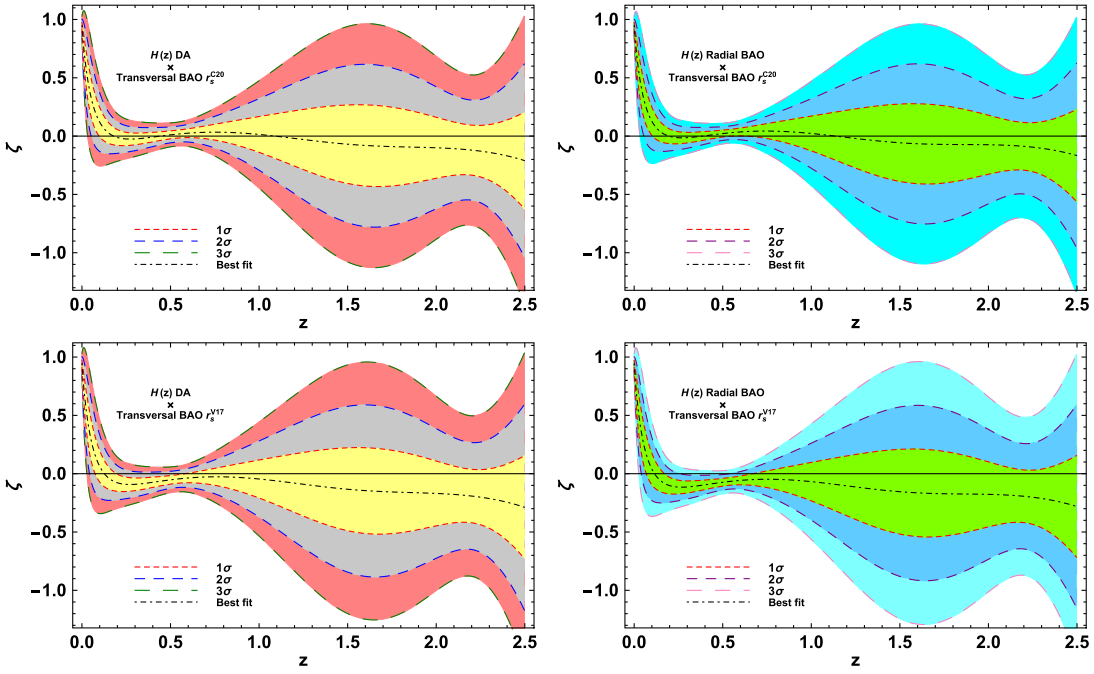


FIG. 2. The distribution of deviations from FLRW assumption $\zeta(z)$ obtained from the Hubble measurements of DA method (left panel) and radial BAO measurements (right panel) with the priors $r_{\rm s}^{\rm C20}$ (top) and $r_{\rm s}^{\rm V17}$ (bottom) obtained in a nonparametric way.

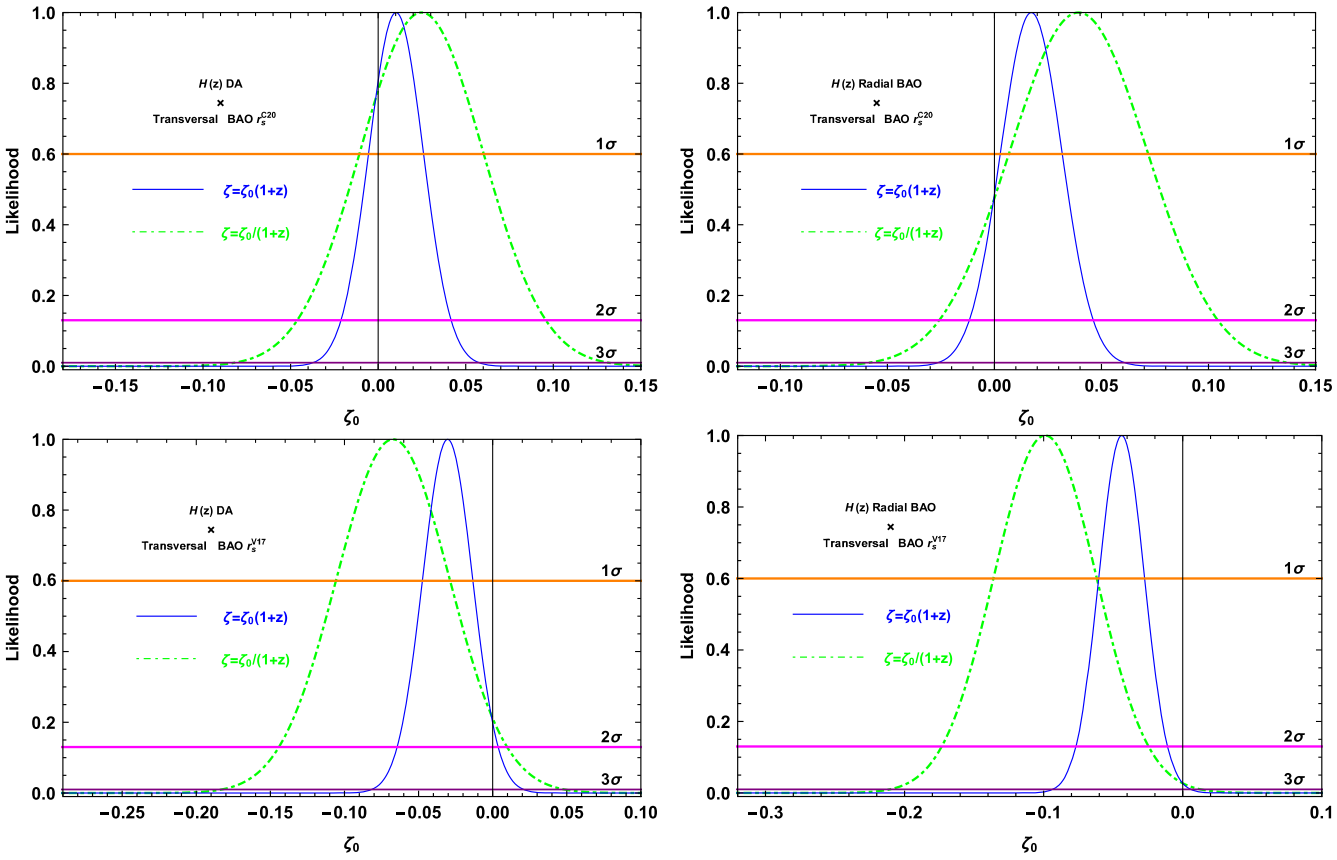


FIG. 3. Likelihood distribution functions obtained from Hubble $H(z)$ measurements of DA method and the transversal BAO observations (left panel) with the priors of $r_s^{C20}$ (top) and $r_s^{V17}$ (bottom). The same cases are from the transversal BAO and Hubble $H(z)$ measurements of radial BAO (right panel).

measurements, and then marginalize its influence with a flat prior in the analysis. The likelihood distribution $\chi'^2$ can be rewritten as

$$\chi'^2(\zeta_0, r_s) = \sum_i^N \frac{\frac{n_i^2}{m_i^2} r_s^2 - 2\frac{n_i}{m_i} r_s + 1}{\sigma'^2_{\zeta_{obs,i}}}, \tag{19}$$

here, $n_i = 1 - \zeta(z_i)$, $m_i = \theta_{BAO,i} D_{C,i}$, and

$$\sigma'^2_{\zeta_{obs,i}} = \left(\frac{\sigma_{\theta_{BAO,i}}}{\theta_{BAO,i}}\right)^2 + \left(\frac{\sigma_{D_{C,i}(z)}}{D_{C,i}(z)}\right)^2. \tag{20}$$

Then, following the method in Refs. [69,77], we marginalize analytically the likelihood function over $r_s$ with the assumption of a flat prior on $r_s$, and rewrite the marginalized $\chi'^2_M$ as

TABLE IV. The summary of maximum likelihood estimation results of $\zeta_0$ for the two parametrizations. The $\zeta_0$ is represented by the best fit value $\zeta_{0,best} \pm 1\sigma \pm 2\sigma \pm 3\sigma$ for each dataset. $1\sigma$, $2\sigma$, and $3\sigma$ denote the 68.3%, 95.4%, and 99.7% CL, respectively. The superscripts A and B represent the cases obtained from Hubble $H(z)$ measurements of the DA method and the radial BAO observation, respectively. The superscripts $\diamond$, $\star$, and $\dagger$ represent the results obtained with the priors of $r_s^{C20}$ (two top lines), the priors of $r_s^{V17}$ (two middle lines), and flat priors of $r_s$ (two bottom lines), respectively.

| | P1: $\zeta_0(1+z)$ | $\chi^2_{red}$ | P2: $\zeta_0 \frac{1}{1+z}$ | $\chi^2_{red}$ |
|---|---|---|---|---|
| $\zeta_0^{A\diamond}$ | $0.010 \pm 0.016 \pm 0.031 \pm 0.049$ | 0.292 | $0.025 \pm 0.036 \pm 0.071 \pm 0.107$ | 0.287 |
| $\zeta_0^{B\diamond}$ | $0.017 \pm 0.015 \pm 0.029 \pm 0.044$ | 0.334 | $0.039 \pm 0.033 \pm 0.066 \pm 0.099$ | 0.331 |
| $\zeta_0^{A\star}$ | $-0.030 \pm 0.017 \pm 0.035 \pm 0.053$ | 0.272 | $-0.067 \pm 0.039 \pm 0.077 \pm 0.117$ | 0.281 |
| $\zeta_0^{B\star}$ | $-0.044 \pm 0.017 \pm 0.033 \pm 0.051$ | 0.308 | $-0.099 \pm 0.038 \pm 0.075 \pm 0.101$ | 0.308 |
| $\zeta_0^{A\dagger}$ | $-0.001 \pm^{0.075}_{0.091} \pm^{0.131}_{0.212} \pm^{0.180}_{0.391}$ | 0.439 | $0.019 \pm^{0.202}_{0.228} \pm^{0.346}_{0.569} \pm^{0.463}_{1.100}$ | 0.439 |
| $\zeta_0^{B\dagger}$ | $0.011 \pm^{0.066}_{0.085} \pm^{0.123}_{0.194} \pm^{0.168}_{0.340}$ | 0.503 | $-0.015 \pm^{0.170}_{0.259} \pm^{0.313}_{0.600} \pm^{0.432}_{1.110}$ | 0.505 |

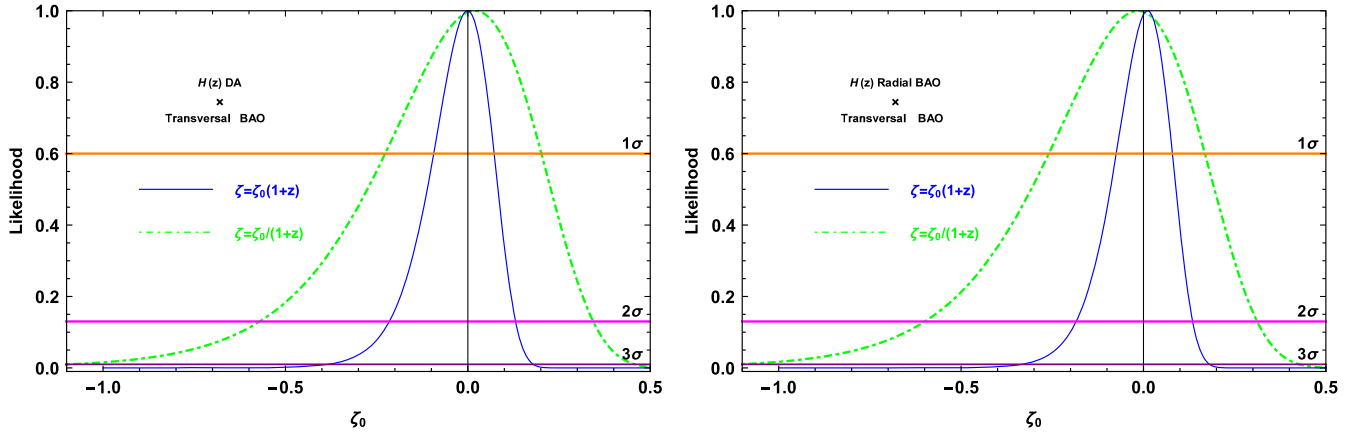


FIG. 4. Likelihood distribution functions obtained from Hubble $H(z)$ measurements of DA method and the transversal BAO observations (left panel) with a flat prior of $r_s$. The same cases are from the transversal BAO and Hubble $H(z)$ measurements of radial BAO (right panel).

$$\chi'^2_M(\zeta_0) = C - \frac{B^2}{A} + \ln\frac{A}{2\pi}, \tag{21}$$

where $A = \sum n_i^2/(m_i^2\sigma'^2_{\zeta_{\mathrm{obs},i}})$, $B = \sum n_i/(m_i\sigma'^2_{\zeta_{\mathrm{obs},i}})$, and $C = \sum 1/\sigma'^2_{\zeta_{\mathrm{obs},i}}$. It should be noted that we adopt the current form of $\zeta(z)$ in Eq. (13) (rather than the form in Ref. [17]) to obtain an analytical expression in Eq. (21) while marginalizing over $r_s$. The free parameter in this equation is $\zeta_0$, and the number of degree of freedom is 1, since the parameter $r_s$ has been marginalized. The results are shown in Fig. 4 and Table IV.

## III. RESULTS AND ANALYSIS

For the reconstructed results obtained from the deviations of the FLRW metric with the nonparametrization method, seen from Fig. 2, the divergence of $\zeta(z)$ in the redshift range $z < 0.1$ may result from the absence of the observed transversal BAO data points. Using the priors of $r_s^{C20}$ and $r_s^{V17}$, the FLRW metric is consistent with the Hubble $H(z)$ measurements from DA method and the transversal BAO observation at $1\sigma$ and $2\sigma$ confidence level (CL), respectively. And no deviation from the FLRW metric can be found for the Hubble $H(z)$ measurements of radial BAO and the transversal BAO observations at $2\sigma$ and $3\sigma$ CL, respectively. Our result is compatible with that from Ref. [17], in which an isotropic universe was obtained at $1\sigma$ CL and $2\sigma$ CL from different reconstruction methods and the priors on the $r_s$ and $H_0$. It also shows that the deviation from the FLRW metric is less than that obtained from Ref. [18], in which a mild deviation of the FLRW metric was found at $3.5\sigma$ CL under the assumptions of $r_s^{C20}$ and $H_0 = 73.4 \pm 1.4\ \mathrm{km\,s^{-1}\,Mpc^{-1}}$ priors. The greater deviation found in Ref. [18] is due to the value of $H_0$ being larger than that in our analysis. In Fig. 2, it can also be seen that the deviation from the FLRW metric obtained from the prior of the sound horizon scale $r_s^{V17}$ is greater than that obtained from the prior $r_s^{C20}$, because a larger value of $r_s$ may result in a larger angular distance $D_A$, as shown in Sec. II C. Thus, bias may be caused by the priors of the sound horizon scales in the test of the FLRW metric. It can be also found that the best-fit value of function $\zeta(z)$ varies with the redshift $z$ regardless of the observational data and the priors on $r_s$.

For the constraints on the parameter $\zeta_0$ by comparing the Hubble $H(z)$ measurements from the DA method with the transversal BAO observation, seen from Fig. 3 and Table IV, we find that the FLRW metric is consistent with the observational data with the priors of $r_s^{C20}$ and $r_s^{V17}$ at $1\sigma$ and $2\sigma$ CL, respectively. And the FLRW metric is also consistent with the Hubble $H(z)$ measurements from the radial BAO and transversal BAO observations with the priors of $r_s^{C20}$ and $r_s^{V17}$ at $2\sigma$ and $3\sigma$ CL, respectively. For the two observational datasets and priors of $r_s$, the error bars obtained from parametrization P1 are nearly 50% smaller than those from parametrization P2, although the results are almost independent on the parametrizations of $\zeta(z)$. It should be noted that the results from the parametrizations are consistent with the results from the nonparametrization method. Thus, the parametric method provides an effective way to check the consistency relation through constraining the parameter $\zeta_0$. In addition, the constraints obtained from the priors of $r_s^{V17}$ imply the greater violation from the FLRW metric than that from priors of $r_s^{C20}$, which is similar to the results obtained from the nonparametric method. Therefore, for nonparametric and parametric methods, priors of the sound horizon scale will lead to bias in the tests of the FLRW metric, if the exact value of $r_s$ cannot be given from astronomical observations.

As for the case of constraints on the parameter $\zeta_0$ with a flat prior of the sound horizon scale $r_s$, the FLRW metric is compatible with the observational data at $1\sigma$ CL, although

the error bars are much larger (nearly 5 times) than those obtained with the priors of the specific $r_s$. While comparing the two compilations of Hubble measurements with the transversal BAO data, the error bars obtained from parametrization P1 are nearly 60% smaller than those from parametrization P2. So, parametrization P1 offers a better fit on the observational data. The value of the reduced $\chi^2$ ($\chi^2_{\rm red}$) obtained from the flat prior of $r_s$ is closer to 1 than that from the prior of $r_s$. Thus, the constraint obtained from the flat prior of $r_s$ provides the better fit for the observational measurements than that from the priors of $r_s$. It should be noted that the value of $\chi^2_{\rm red}$ is below 1. Therefore, this indicates some overfitting, which may reduce the statistical significance of these results. In addition, the method in our analysis is independent of any cosmological model, except that the radial BAO measurements are obtained under the assumption of ΛCDM. Therefore, using the Hubble measurements from the differential age method and the transversal BAO measurements, the method for testing the FLRW metric is not only independent of the cosmological model, but also independent of the priors of the values of the sound horizon scale $r_s$.

## IV. CONCLUSION AND DISCUSSION

The *CP* is one of the two fundamental assumptions of the SCM, and it is the cornerstone of measuring cosmic distances and clocks through the FLRW metric. It is significant to verify the FLRW metric with new methods and astronomical observations, because any deviations from the FLRW metric may imply that the tension in the SCM might be caused by an oversimplifying formulation of its fundamental assumptions.

The comoving observed angular modes from the Hubble $H(z)$ measurements and transversal BAO data should be consistent with each other across the expansion history of the Universe, if the space time of our Universe is described by the FLRW metric. Thus, the direct detections of Hubble $H(z)$ measurements and transversal BAO data provide us with the opportunity to test the FLRW metric. In this work, following the nonparametric method in Refs. [17,18], we first test the FLRW metric by comparing the Hubble $H(z)$ measurements obtained from the differential age method (or determination of the BAO peak in the radial direction) with transversal BAO measurements. The function $\zeta(z) = 1 - \theta_{\rm BAO}/\theta_{H(z)}$ is adopted to probe the possible deviations from the FLRW metric. We use the best-fitted sound horizon scale $r_s$ from the transversal BAO mode at the low redshift and the value of $H_0$ reconstructed from the Hubble measurements to derive the ADDs. The function $\zeta(z)$ at any redshift are obtained with the Gaussian process. The results show that FLRW metric is consistent with the observations regardless of the priors of the sound horizon scale, and the observational data favors a function $\zeta(z)$ varying with redshift. It can be also concluded that the deviation from the FLRW metric is dependent on the priors on the sound horizon scale $r_s$, since a smaller value of $r_s$ may result in a smaller ADD.

Then, we employ two parametrizations to describe the function $\zeta(z)$ that evolves with the redshift $z$, namely, $\zeta(z) = \zeta_0(1+z)$ (P1) and $\zeta(z) = \zeta_0/(1+z)$ (P2), and test the FLRW metric by constraining the parameter $\zeta_0$ under the priors of sound horizon scale. Our results show that P1 offers a much more rigorous constraint on the parameter $\zeta_0$ than P2. Compared with the results from the nonparametric method, the same results are obtained from the parametric method for the observational data and the priors of the sound horizon scale $r_s$. Therefore, the parametric method offers an effective way to test the FLRW metric by constraining the parameter $\zeta_0$. The results also imply that in the test of the FLRW metric, some bias might be caused by the priors of the sound horizon scale $r_s$ when the exact value of observation $r_s$ is not determined.

To test the FLRW metric independent of the sound horizon scale $r_s$, we consider a fiducial value of $r_s$ as a nuisance parameter to determine the ADD $D_A$ from transversal BAO data, and then marginalize its influence with a flat prior in the analysis. Results show that the FLRW metric is compatible with the observational data at $1\sigma$ CL, although the ability to constrain the parameter $\zeta_0$ is weaker than that obtained from the priors of the sound horizon scale $r_s$. Furthermore, the method to test the FLRW metric with the Hubble measurements from the differential age method is independent of any cosmological model. Due to the limited observed data available and its large error at present, the ability to constrain the parameter $\zeta_0$ is weak in this work. With the developments of powerful optical and radio telescopes, we can better measure the Hubble parameter using the cosmic chronometer and BAO methods. In addition, the neutral hydrogen intensity mapping technique can be used to measure the BAO signals more efficiently, and 200 observational data at $0 < z < 2.5$ will be realized in the coming decades [78]. So, in the following work, simulation data can be used to detect the ability of future observational data to test the FLRW metric. As the quality and quantity of measurements for future Hubble and BAO measurements increase, the parametric method in our analysis will be a powerful way to test the consistency relation both independent of the cosmological model and the sound horizon scale.

## ACKNOWLEDGMENTS

We very much appreciate helpful comments and suggestions from anonymous referees, and helpful discussion from Hongwei Yu, Puxun Wu, and Zhengxiang Li. This work was supported by the National Natural Science

Foundation of China under Grants No. 12375045, No. 12305056, No. 12105097 and No. 12205093; the Hunan Provincial Natural Science Foundation of China under Grants No. 12JJA001 and No. 2020JJ4284; the Natural Science Research Project of Education Department of Anhui Province No. 2022AH051634, the Science Research Fund of Hunan Provincial Education Department No. 21A0297.

[1] A. G. Riess *et al.*, Astron. J. **116**, 1009 (1998).
[2] S. Perlmutter *et al.*, Astrophys. J. **517**, 565 (1999).
[3] N. Aghanim, Y. Akrami, M. Ashdown *et al.* (Planck Collaboration), Astron. Astrophys. **641**, A6 (2020).
[4] D. M. Scolnic, D. O. Jones, A. Rest *et al.*, Astrophys. J. **859**, 101 (2018).
[5] S. Alam, M. Aubert, S. Avila *et al.*, Phys. Rev. D **103**, 083533 (2021).
[6] C. Heymans, T. Tröster, M. Asgari *et al.*, Astron. Astrophys. **646**, A140 (2021).
[7] T. M. C. Abbott, M. Aguena, A. Alarcon *et al.*, Phys. Rev. D **105**, 023520 (2022).
[8] L. F. Secco, S. Samuroff, E. Krause *et al.*, Phys. Rev. D **105**, 023515 (2022).
[9] P. K. Aluri, P. Cea, P. Chingangbam *et al.*, Classical Quantum Gravity **40**, 094001 (2023).
[10] C. Krishnan, R. Mohayaee, E. Ó Colgáin, M. M. Sheikh-Jabbari, and L. Yin, Classical Quantum Gravity **38**, 184001 (2021).
[11] D. A. Díaz-Pachón, O. Hössjer, and R. J. Marks II, Found. Phys. **53**, 1 (2023).
[12] S. Weinberg, Rev. Mod. Phys. **61**, 1 (1989).
[13] V. Sahni and A. A. Starobinsky, Int. J. Mod. Phys. D **09**, 373 (2000).
[14] A. G. Riess, S. Casertano, W. Yuan, L. M. Macri, and D. Scolnic, Astrophys. J. **876**, 85 (2019).
[15] G. Efstathiou, Mon. Not. R. Astron. Soc. **505**, 3866 (2021).
[16] R. Maartens, Trans. R. Soc. A **369**, 5115 (2011).
[17] R. Arjona and S. Nesseris, Phys. Rev. D **103**, 103539 (2021).
[18] C. Bengaly, Phys. Dark Universe **35**, 100966 (2022).
[19] G. C. Carvalho, A. Bernui, M. Benetti, J. C. Carvalho, E. de Carvalho, and J. S. Alcaniz, Astropart. Phys. **119**, 102432 (2020).
[20] L. Verde, J. L. Bernal, A. F. Heavens *et al.*, Mon. Not. R. Astron. Soc. **467**, 731 (2017).
[21] G. F. R. Ellis and W. Stoeger, Classical Quantum Gravity **4**, 1697 (1987).
[22] B. Roukema, T. Buchert, J. J. Ostrowski, and M. J. France, Mon. Not. R. Astron. Soc. **448**, 1660 (2015).
[23] B. Roukema, T. Buchert, H. Fuji, and J. J. Ostrowski, Mon. Not. R. Astron. Soc. **456**, L45 (2016).
[24] X. Ding, M. Biesiada, S. Cao, Z. Li, and Z.-H. Zhu, Astrophys. J. Lett. **803**, L22 (2015).
[25] X. Zheng, X. Ding, M. Biesiada, S. Cao, and Z.-H. Zhu, Astrophys. J. **825**, 17 (2016).
[26] P. A. R. Ade *et al.*, Astron. Astrophys. **594**, A13 (2016).
[27] C. L. Bennett *et al.*, Astrophys. J. Suppl. Ser. **208**, 20 (2013).
[28] R. Jimenez and A. Loeb, Astrophys. J. **573**, 37 (2002).
[29] C. Zhang, H. Zhang, S Yuan, S. Liu, T.-J. Zhang, and Y.-C. Sun, Res. Astron. Astrophys. **14**, 1221 (2014).
[30] D. Stern, R. Jimenez, L. Verde, M. Kamionkowski, and S. A. Stanford, J. Cosmol. Astropart. Phys. 02 (2010) 008.
[31] M. Moresco, A. Cimatti, R. Jimenez *et al.*, J. Cosmol. Astropart. Phys. 08 (2012) 006.
[32] M. Moresco, L. Pozzetti, A. Cimatti, R. Jimenez, C. Maraston, L. Verde, D. Thomas, A. Citro, R. Tojeiro, and D. Wilkinson, J. Cosmol. Astropart. Phys. 05 (2016) 014.
[33] A. L. Ratsimbazafy, S. I. Loubser, S. M. Crawford, C. M. Cress, B. A. Bassett, R. C. Nichol, and P. Väisänen, Mon. Not. R. Astron. Soc. **467**, 3239 (2017).
[34] M. Moresco, Mon. Not. R. Astron. Soc. **450**, L16 (2015).
[35] L. Yang, H. Yu, and P Wu, Astrophys. J. Lett. **946**, L49 (2023).
[36] V. Marra and D. Sapone, Phys. Rev. D **97**, 083510 (2018).
[37] P. Wu and H. Yu, Phys. Lett. B **644**, 16 (2007).
[38] E. Gaztanaga, A. Cabre, and L. Hui, Mon. Not. R. Astron. Soc. **399**, 1663 (2009).
[39] J. Magaña, M. H Amante, M. A. Garcia-Aspeitia, and V. Motta, Mon. Not. R. Astron. Soc. **476**, 1036 (2018).
[40] C. Blake, S. Brough, M. Colless *et al.*, Mon. Not. R. Astron. Soc. **425**, 405 (2012).
[41] A. Oka, S. Saito, T Nishimichi, A. Taruya, and K. Yamamoto, Mon. Not. R. Astron. Soc. **439**, 2515 (2014).
[42] S. Alam, M. Ata, S. Bailey *et al.*, Mon. Not. R. Astron. Soc. **470**, 2617 (2017).
[43] Y. Wang, G. Zhao, C. Chuang *et al.*, Mon. Not. R. Astron. Soc. **469**, 3762 (2017).
[44] C.-H. Chuang and Y. Wang, Mon. Not. R. Astron. Soc. **435**, 255 (2013).
[45] J. E. Bautista, J. Guy, J. Rich *et al.*, Astron. Astrophys. **603**, A12 (2017).
[46] T. Delubac, J. E. Bautista, N. G. Busca *et al.*, Astron. Astrophys, **574**, A59 (2015).
[47] L. Anderson, E. Aubourg, S. Bailey *et al.*, Mon. Not. R. Astron. Soc. **439**, 83 (2014).
[48] A. Font-Ribera, D. Kirkby, N. Busca *et al.*, J. Cosmol. Astropart. Phys. 05 (2014) 027.
[49] G. C. Carvalho, A. Bernui, M. Benetti, J. C. Carvalho, and J. S. Alcaniz, Phys. Rev. D **93**, 023530 (2016).
[50] J. S. Alcaniz, G. C. Carvalho, A. Bernui, J. C. Carvalho, and M. Benetti, in *Gravity and the Quantum*, edited by J. Bagla and S. Engineer, Fundamental Theories of Physics Vol. 187 (Springer, Cham, 2017).
[51] E. de Carvalho, A. Bernui, G. C. Carvalho, C. P. Novaes, and H. S. Xavier, J. Cosmol. Astropart. Phys. 04 (2018) 064.
[52] R. C. Nunes, S. K. Yadav, J. F. Jesus, and A. Bernui, Mon. Not. R. Astron. Soc. **497**, 2133 (2020).

[53] D. G. York *et al.* (SDSS Collaboration), Astrophys. J. **120**, 1579 (2000).
[54] E. D. Carvalho, A. Bernui, F. Avila, C. P. Novaes, and J. P. Nogueira-Cavalcante, Astron. Astrophys. **649**, A20 (2021).
[55] M. Seikel, S. Yahya, R. Maartens, and C. Clarkson, Phys. Rev. D **86**, 083001 (2012).
[56] S. Yahya, M. Seikel, C. Clarkson, R. Maartens, and M. Smith, Phys. Rev. D **89**, 023503 (2014).
[57] J. E. Gonzalez, J. S. Alcaniz, and J. C. Carvalho, J. Cosmol. Astropart. Phys. 04 (2016) 016.
[58] S. Santos-da-Costa, V. C. Busti, and R. F. L. Holanda, J. Cosmol. Astropart. Phys. 10 (2015) 061.
[59] P. Mukherjee and N. Banerjee, Eur. Phys. J. C **81**, 1 (2021).
[60] R. F. L. Holanda, J. C. Carvalho, and J. S. Alcaniz, J. Cosmol. Astropart. Phys. 04 (2013) 027.
[61] L. Verde, P. Protopapas, and R. Jimenez, Phys. Dark Universe **5–6**, 307 (2014).
[62] Z. Li, J. E. Gonzalez, H. Yu, Z.-H. Zhu, and J. S. Alcaniz, Phys. Rev. D **93**, 043014 (2016).
[63] V. C. Busti, C. Clarkson, and M. Seikel, Mon. Not. R. Astron. Soc. **441**, L11 (2014).
[64] H. Zhang, Y.-C. Wang, T.-J. Zhang, and T. Zhang, Astrophys. J. Suppl. Ser. **266**, 27 (2023).
[65] C. A. P. Bengaly, Mon. Not. R. Astron. Soc. **499**, L6 (2020).
[66] A. Shafieloo, A. G. Kim, and E. V. Linder, Phys. Rev. D **85**, 123530 (2012).
[67] M. Seikel, C. Clarkson, and M. Smith, J. Cosmol. Astropart. Phys. 06 (2012) 036.
[68] T. M. Abbott, S. Desai, and F. B. Abdalla, Mon. Not. R. Astron. Soc. **480**, 3879 (2018).
[69] B. Xu *et al.*, Astrophys. J, **939**, 115 (2022).
[70] Z. Li, P. Wu, and H. Yu, Astrophys. J. **729**, L14 (2011).
[71] X. L. Meng, T. J. Zhang, and H. Zhan, Astrophys. J. **745**, 98 (2012).
[72] T. Yang, R. F. L. Holanda, and B. Hu, Astropart. Phys. **108**, 57 (2019).
[73] X. Fu, L. Zhou, and J. Chen, Phys. Rev. D **99**, 083523 (2019).
[74] L. Zhou, X. Fu, Z. Peng, and J. Chen, Phys. Rev. D **100**, 123539 (2019).
[75] X. Fu, J. Yang, Z. Chen, L. Zhou, and J. Chen, Eur. Phys. J. C **80**, 893 (2020).
[76] K. Liao, Z. Li, S. Cao, M. Biesiada, X. Zheng, and Z.-H. Zhu, Astrophys. J. **822**, 74 (2016).
[77] A. Conley, J. Guy, M. Sullivan *et al.*, Astrophys. J. Suppl. Ser. **192**, 1 (2011); P. Bull, P. G. Ferreira, P. Patel, and M. G. Santos, Astrophys. J. **803**, 21 (2015).
[78] M. Zhang, B. Wang, P.-J. Wu, J.-Z. Qi, Y. Xu, J.-F. Zhang, and X. Zhang, Astrophys. J. **918**, 56 (2021); P.-J. Wu and X. Zhang, J. Cosmol. Astropart. Phys. 01 (2022) 060.